Proceedings of the ASME 2012 International Mechanical Engineering Congress and Exposition
IMECE2012
November 9-15, 2012, Houston, Texas, USA

IMECE2012-88788

AIRFOIL OPTIMIZATION FOR SMALL WIND TURBINES USING MULTI OBJECTIVE GENETIC ALGORITHM

KRISHNIL R RAM
The University of the South Pacific
Suva , Fiji
ram_k@usp.ac.fj

SUNIL LAL
The University of the South Pacific
Suva, Fiji
lal_s@usp.ac.fj

M RAFIUDDIN AHMED
The University of the South Pacific
Suva, Fiji
rafiuddinm.ahmed@usp.ac.fj

ABSTRACT

Small wind turbines are gaining popularity due to their ability to meet community or domestic needs in isolated areas with relatively easier installation and lower cost than large wind turbines. This study looks at optimizing airfoils for use in small horizontal axis wind turbines. The optimization looks to maximize the lift coefficient (C_l) while minimizing or fixing the drag coefficient (C_d). To satisfy these two objectives a multi – objective genetic algorithm is used. The airfoil is parameterized using a composite Bezier curve with two Bezier segments and 11 control points. Appropriate curvature conditions are implemented at the leading and trailing edge of the airfoil and geometric constraints are applied to maintain the maximum thickness between 8% to 14% of the chord for structural reasons. An existing genetic algorithm (GA) code is modified in C++ to generate suitable airfoils using the 13 control points and pass the coordinates to a solver for analysis. As a result four new airfoils are generated for application in low Reynolds number (Re) flow. The characteristics and suitability of the four airfoils are discussed while comparing them to the popular SG6043 airfoil.

INTRODUCTION

With rapidly increasing fuel prices and demand for energy, the South Pacific is looking at a possible energy crisis if it does not inititate R & D of renewable energy devices. One of the more mature technologies in renewable energy is wind energy. The South Pacific Islands have a unique challenge in that most the populations are spread across the ocean in hundreds of islands. While mega-watt class hydro and wind installations can cater for main islands and population centers, small wind turbines (SWT) are a perfect solution for outer island usage. SWT's range from a few watts to a 100kW(1). This scale allows the use of SWT's as village power sources and even be integrated into national grids. SWT's can also be mounted on buildings and near homes for personal or mini-grid applications. While the potential for SWT's are being realized worldwide, the SWT's have not yet become as cost effective as their mega watt class counterparts. The European Wind Energy Association (EWEA) has pointed out that there are a number of components of SWT's that need to be improved in order to reduce its cost per kW and make this technology more economical. A major issue reported by EWEA is the need for improved airfoil shapes; variable chord distribution and variable twist distribution such that the performance of the SWT can be improved significantly (1). As the airfoil is at the forefront of energy extraction from the wind, the importance of designing efficient and structurally sound blade sections cannot be overemphasized. Since small wind turbines have a smaller chord and operate at lower speeds, these turbines can be classed as operating at low Reynolds numbers. Even though there is no fixed Reynolds number range that bounds the low Reynolds regime, the term low Reynolds number has also come to mean the flow regime where the chord Reynolds number is below approximately 500,000(2). The main focus in the design of blade sections has been to maximize lift : drag ratio (L/D) mainly by increasing the lift coefficient (C_l) (3). The commonly used NACA airfoils are not appropriate for wind turbines that need to operate in regions of low wind (4). NACA airfoils are suitable mainly for high Reynolds numbers and relatively small angles of attack (α)(5). Wind turbine airfoils need to be stable at a wide range of angles of attack. This means that the L/D ratio should not drop abruptly with α change. While numerous airfoils have been developed for high Reynolds number wind turbines, the development in airfoils for small wind turbines has been minimal. Giguere and Selig presented the SG60X family of airfoils suitable for small wind turbine applications (6). Apart from these only a few airfoils are suited to small wind turbines. This study is aimed at adding new airfoils to the already existing collection of small wind turbine airfoils. Airfoil design can be grouped in two main categories, direct design and inverse design. Direct airfoil design using numerical optimization (7) is common and involves manipulating the curves that define the airfoil to achieve desired characteristics. The inverse design approach (8), which involves generating airfoils to match velocity distributions, can also employ optimization. With the advances in processing powers of computers, optimization of airfoils allows for creation of new airfoils for specialized applications. Genetic Algorithm (9) optimization is a proven, robust method which utilizes nature's process of evolution to generate optimum solutions. The objective of this study is to design new airfoils for small wind turbines using genetic algorithm optimization. A brief review of airfoil parameterization and optimization techniques is done to explore the possible methods available. Four new airfoils along with their characteristics are presented.

OBJECTIVE FUNCTIONS

The objective of the algorithm was to maximize the lift while minimizing or fixing the drag. Two distinct cases were considered for optimization. The first case was for a single *α* while the second involved optimizing at multiple *α*. For case 1, the following objectives were set:

Minimize drag coefficient (C_d), Maximize (C_l) for α =10° and α = 8°

And gives the following fitness function:

$$F(B(u),\mathrm{Re}) = C_l + 0.001/C_d + 0.001 \quad (1)$$

For case 2 the objectives were
Minimize (C_d), Maximize (C_l) for α_i ..... α_n
And gives the following generalized fitness function:

$$F(B(u),\mathrm{Re}) = \sum_{i=1}^{n}\left(\frac{Cl_i}{Cd_i}\right)\times\frac{1}{n} \quad (2)$$

Where n is the number of angles. For case 2 the α range was from 0 to 13° with increments of 0.5°. The Reynolds number chosen for optimization was 300,000.

AIRFOIL PARAMETERIZATION

Before optimization can be applied to a problem, it needs to be defined as a mathematical model taking into account all variables and parameters. In order to optimize the airfoil, the 2D shape of the airfoil needs to be parameterized by defining the variables that will control the coordinates and shape of the airfoil. Numerous airfoil parameterization methods have been proposed. In this study the need was for a single discipline shape parameterization scheme whereby only the shape function will be parameterized. Samareh (10) provides a detailed review of multidisciplinary parameterization for airfoils. The choice of parameterization depends on the needs of the design problem. Efficient airfoil parameterization schemes has been a subject of ongoing research. The simplest representation of an airfoil is to simply define a sufficient number of x coordinates and the corresponding y coordinates. A large number of (x,y) points are required to approximate the curvature of the airfoil. The discrete y coordinates are joined together as a continuous curve to form the airfoil. In this manner a very flexible parameterization is obtained; however great care must be taken to preserve the smoothness and reasonable shape of the airfoil (11). This method also creates a large number of control variables which would prove computationally expensive to optimize. Helmut Sobieczky (12) proposed a method with ideally low number of control points called the PARSEC parameterization scheme. The PARSEC scheme utilizes the 11 geometric characteristics of the airfoil as control parameters. These control parameters are the leading edge radius, upper crest position and curvature, lower crest position and curvature, trailing edge direction, trailing edge wedge thickness, trailing edge wedge angle and trailing edge offset. By controlling these variables the upper and lower surfaces of the airfoil are generated. The PARSEC method generates realistic airfoil shapes which are easily interpreted by flow solvers and allow for easy convergence. While the PARSEC method is specifically created for airfoil shape generation, it limits the possibility of airfoil shapes especially at the leading edge as mentioned by (13). Also, this method may lead to overlapping of the upper and lower surface i.e it does not guarantee a physically acceptable trailing edge (14). Recently Derksen and Rogalsky have proposed the PARSEC –Bezier parameterization scheme (15). This method has been developed to reduce the non-linear interaction of the parameters and create a more direct link of the parameters to the objective function. Airfoil parameterization using B-Splines (Basis splines) is also common as demonstrated in (7) and (16). Similar to Bezier curves, B-splines are constructed using a parameter u and control points. B-Splines have a much better local control as compared to Bezier curves. Originally inspired by thin wooden 'splines' used in ship design, B-Splines can be considered as a series of Bezier curves connected in such a way that continuity is maintained throughout the curve. B-splines require the calculation of basis functions through recurrence. The de Boor algorithm is normally used to evaluate B-splines. One of the most common and easiest ways to represent free form curves is via Bezier curves. Bezier curves were developed by Paul de Faget de Casteljau (17) and later popularized by Pierre Bezier. Bezier curve parameterization allows the use of a parameter u, and multiple control points $\boldsymbol{P}_i$ to generate x and y coordinates of an airfoil. This study makes use of Bezier curves to parameterize the airfoil. Several studies (8, 18, 19) have used Bezier airfoil parameterization for airfoil optimization. The Bezier parameterization scheme is easy to implement along with constraints and has reasonable accuracy. The order of the Bezier curve is determined by the number of control points. For $n + 1$ control points $\boldsymbol{P_i}$, a Bezier curve of the *nth* order will be formed. By joining the control points together, a control polygon is formed. The generalized form of a Bezier curve is defined as:

$$\mathbf{B}(u) = \sum_{i=0}^{n} \mathbf{P}_i \frac{n!}{i!(n-i)!} u^i (1-u)^{n-i} \quad , u \in (0,1) \quad (3)$$

Where $\boldsymbol{B}$ *(u)* vector contains the x and y coordinates on the curve and $\boldsymbol{P}_i$ contains the x, y coordinates of the control polygon. The parameter u is defined from 0 to 1 uniformly in this study. For this study a composite Bezier curve was used to define the geometry of the airfoil. One Bezier curve was used to represent the upper surface while a second Bezier curve was used to represent the lower surface as shown in Figure 1.

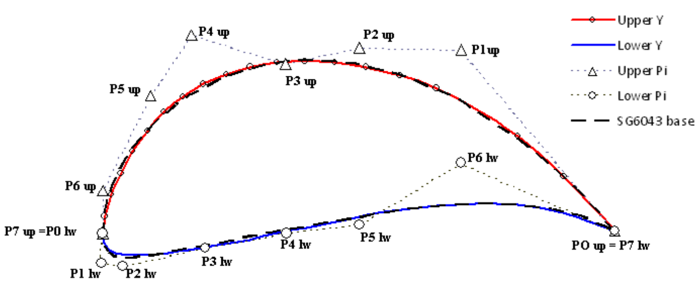

Fig 1: Bezier curve parameterization of SG6043(6) airfoil using composite Bezier curves , *up* = upper surface, *lw* = lower surface. Points *P* were achieved through interpolation.

The start and end control points, *PO* and *P7* lie on the airfoil curve itself at the leading and trailing edges and their positions are fixed to maintain a chord length of unity for easier computation and comparison in the flow solver XFOIL. Specific conditions were defined to control the integrity of the airfoil shape at the leading and trailing edge. At the leading edge the initial and terminal points of the upper and lower curves coincide to close the curve. C^0 continuity is enforced at the trailing edge by simply connecting the upper and lower curve points without any special condition. At the leading edge, C^1 continuity was enforced by ensuring that *P1 lw* is a reflection of *P6 up* with the mirror line being perpendicular to segment *P1 lw – P6 up* and crossing at *P7 up*. Despite the leading and trailing edges being fixed, the upper and lower surfaces of the airfoil had a large degree of freedom and had the possibility to represent a suitably large number of free form closed shapes. With the leading and trailing points restricted and *P1 lw* being governed by the coordinates of *P6 up*, a total of 11 control points were available to manipulate the airfoil shape. Higher order (10^{th}) curves were also experimented on but these had increased number of control points and were prone to form bumps due to enhanced local control which was not taken well by the geometry sensitive solver. The 7^{th} order Bezier airfoil parameterization function was coded in C++. Geometric constraints on the airfoil ensured that only realistic airfoil shapes were analyzed. The constraints are looked at later in the paper.

OPTIMIZATION SCHEME

The problem of increase lift and other favorable characteristics of an airfoil while minimizing or maintaining drag and other unwanted traits calls for a suitable multi – objective optimization scheme. Airfoil shape optimization gives a rapid indication of the possible directions for improvement when direct or inverse geometric cut-and-try is impractical (20). Gradient based optimization models have been used (21) for optimization in aerodynamics. This method requires the gradient of the objective function with respect to the shape parameter (22).The use of neural network models to solve airfoil shape optimization issues have been explored by (23, 24) and others. The Artificial Neural Network technique copy's the functioning of the human brain by using artificial neuron connections to recognize complex patterns between input and output data. The use of Particle Swarm Optimization (PSO) is also common to optimizations in aerodynamics. The use of PSO in airfoil optimization has been demonstrated by (25) and others. The PSO mimics the characteristics of a flock of birds to gain optimal solutions. The term particle refers to candidate solutions in the PSO algorithm. Particles identify and exploit promising areas of the design space by learning from previous experience and emulating the success of other particles. Evolutionary algorithms are by far the most popular in airfoil optimization. Evolutionary Algorithms (EA) are based on the neo-Darwinism paradigm of evolution. Two common variants of EA in airfoil optimization are Differential Evolution and Genetic Algorithm Optimization. Differential Evolution (DE) was originally developed by Price (26) and is mostly used for real valued functions. This meta-heuristic optimization approach works on generating candidate solution vectors and improving on them through re-combination with other solution vectors from the population. The Genetic Algorithm (GA) optimization approach was developed by Holland (9) and has seen use in numerous optimization problems owing to its robust approach. The GA optimization has been used by Grasso (18) and others (8, 19, 27-29) for airfoil development. The GA is a stochastic algorithm and it keeps in memory a population of solutions during iteration rather than a single solution (30). GA uses a direct analogy of natural behavior. But before GA can be run, a suitable coding (or representation) for the problem must be devised (31). While conventional GA represented the population of solutions in binary bits, recent developments have allowed for real valued GA approach. The solutions of GA are coded as an array of bits called chromosomes or genotype. The genotype represents an individual in a solution vector called the phenotype. GA is an iterative process and each iteration is called a generation. The initial population is made up of individuals solutions represented in chromosomes. Each individual is subjected to a fitness function that will determine its fitness values. Normally the chromosomes with the desired or closer to desired fitness values are chosen to be parents in the next generation. The parents are then mated using crossover methods to form the next population set. A crossover ratio C_r determines the rate of crossover of genes in the parent chromosomes. The fitness function is repeated on the next set of population until a termination condition is reached. The termination condition may be reached if a satisfactory solution is found or at the end of the generations. During selection it is common to use a roulette wheel. Here the selection is made biased by assigning better solution a higher probability of getting selected. Mutation rate is also an important factor in GA. In many cases GA may find a solution which it believes to be the best solution. Even though the solution may have a higher fitness value, this may not be the answer or the very best. However since the roulette wheel will favor this solution, the tendency for the solution to get stuck with local maxima is high. To prevent this from happening mutation is allowed after selection. Here, for a certain number of individuals the bits are flipped randomly (in binary chromosomes). This study utilizes the binary coded GA written in C++ by Lal et al (32). Figure 2 shows the flow of information in the GA optimization. Initialization of the population also includes seeding of the popular SG6043 airfoil control points. Since GA optimizes the control points of the Bezier functions that governed the airfoil shapes, the 11 control points were converted into a bit string of 88 bits. Each control point was represented using 8 bits.

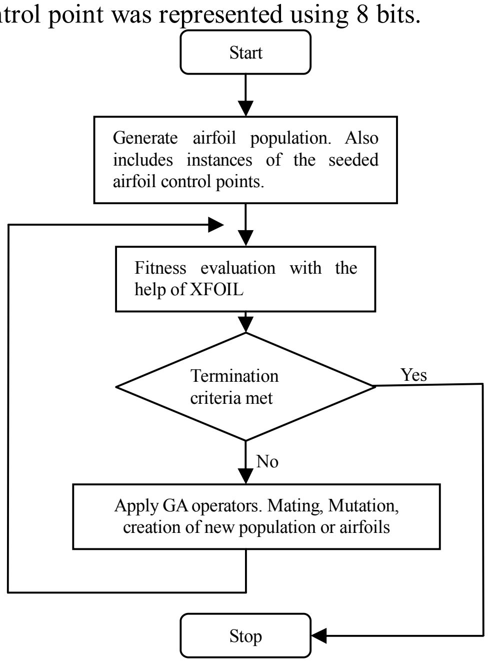

Fig 2: Flowchart for airfoil optimization using GA.

GEOMETRIC CONSTRAINTS AND FITNESS EVALUATION

The flow solver used in this study is highly sensitive to geometry and hence strict geometry conditions are set to prevent unnecessary analysis and failure of analysis by passing non realistic airfoil shapes onto the solver.

To ensure that the upper and lower Bezier curves do not overlap, the following condition was set.

$$Y(u)_{upper} - Y(u)_{lower} > 0 \text{ , (Except for } P0 \text{ and } P7) \quad (4)$$

To maintain structural strength of the wind turbine blade, the blade section must be sufficiently thick. The thickness is controlled between 8 to 14 % of the chord using the following condition.

$$0.14 > (Y(u)_{upper} - Y(u)_{lower}) > 0.08 \quad (5)$$

The upper and lower limit of the y coordinates was set to prevent very highly cambered airfoils and to maintain a realistic search space. The x coordinates were fixed in order to reduce the number of control variables.

$$(Y(u)_{upper}) \leq 0.2 \qquad (Y(u)_{lower}) \geq -0.1 \quad (6)$$

Instead of coding the constraints along with the individual solutions, the solutions are allowed to defy these conditions initially. Once the shapes are created, a pre- fitness evaluation is done and the shapes that are not conforming to any of the geometric conditions are assigned the lowest fitness value of 1 and further analysis of these curves is not permitted. The popular panel method viscous-inviscid flow solver XFOIL(33) was used to calculate the C_l and C_d values of the airfoils at pre-defined Reynolds numbers and α. The C_l and C_d values were input to the fitness function. Figure 3 shows the convergence history of the fitness evaluation in GA for airfoil optimization using composite Bezier parameterization.

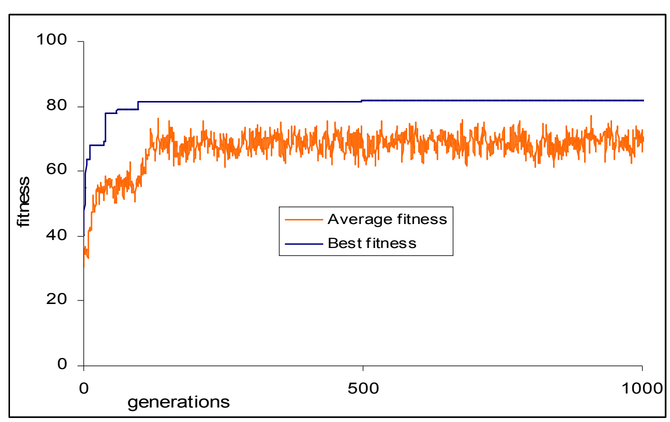

Fig 3: fitness history over several generations for a single run in case 1.

Figure 4 shows the results of the optimization. For case 1, USP03 and USP04 were the results of optimization at angles of 10° and 8° respectively. Following case 2, USP05 was optimized to perform better between 8 to 10° while USP06 was optimized in case 2 to give a higher average L/D from 7 to 13° angle of attack. USP06 is a thick airfoil suitable for the near root region of the blade.

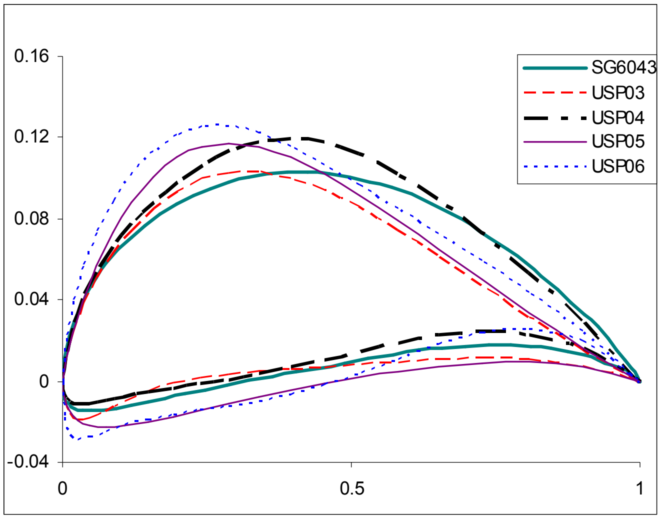

Fig 4: The seeded airfoil SG6043 along with the optimized airfoils USP0X.

AIRFOIL TESTING

Numerical analysis was performed on the USP03 and USP06 airfoils using ANSYS ICEM-CFD and CFX software. Flow over the airfoils was analyzed for different α and Re values. A hexahedral mesh based on O-grid and C-grid topology was created around the foil with 300,000 nodes. The mesh density was increased near the leading and trailing edge to capture the peak suction, stagnation and transition points. A *k-ω* shear stress and transport turbulence model was used. The airfoil was also tested in XFOIL from 0 to 18 degrees. Essential characteristics such as $C_{l,}$ and C_d were noted and compared with CFD and experimental results. An open circuit, suction type low speed wind tunnel was used. The Engineering Laboratory Design (ELD) Inc wind tunnel in the Fluids laboratory at the University of the South Pacific with speed range from 3 m/s to 48.77m/s was used. A centrifugal fan powered by a 10HP AC 3 phase thyristor controlled motor is used to generate the airflow. A maximum velocity resolution of 0.08m.s is achievable in the test section. The test section measures 305mm x 303mm x 1000mm. A traversing pitot-static tube was used to measure the velocity in the wind tunnel test section. The Furness Controls FC0510 digital micro manometer was used to take pressure readings. The USP03 and USP06 profiles were milled out in wood and 30 pressure taps were added on the upper and lower surface. The 3D test profiles of USP03 and USP06 were polished to ensure a smooth surface. A separate profile of each airfoil was milled and finished without any pressure tap. This was for direct lift (L) and drag (D) force measurements. A two component lift and drag dynamometer equipped with a Linear Variable Differential Transformer (LVDT) was used. The dynamometer has an accuracy of 1g (f). the airfoils were tested at Reynolds numbers of 100,000 , 200,000 and 300,000 and the results were compared with XFOIL and CFD results.

RESULTS

Figure 5 shows the C_l values of the airfoils at Reynolds number of 300,000. Results are graphed from 0 to 18° angle of attack. The USP0x airfoils show comparable lift characteristics to the reference airfoil SG6043. USP06 has higher values of C_l , reaching a $C_{l\ max}$ of 2.11 at 15° before stalling. USP04 has a $C_{l\ max}$ of 1.68 before stalling softly. Abruptly stalling airfoils are not desirable. USP03 has a soft stall at 11° while USP05 has the lowest C_l values and stalls earliest at 9.5°. Figure 6 shows the drag polar for each airfoil. While USP06 has the highest $C_{l\ max,}$ the thick (14%) airfoil has higher drag values at most C_l hence this is the reason for the lowered L/D values in Figure 7.

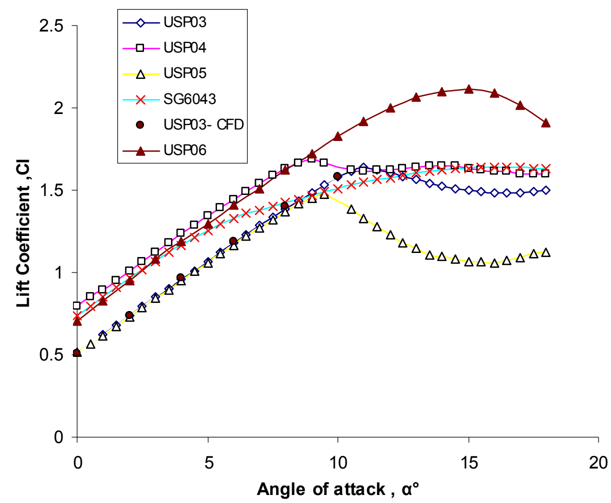

Fig 5: Lift coefficients at Re=300,000

Although the L/D is low compared to SG6043, the L/D ratio is stable from 3 to 13° (Figure 7). This means that the airfoil will perform consistently for a range of flow conditions. This is a desired feature of SWT airfoils. USP03 and USP04, which were optimized for design angles of 8 and 10°, show, improved higher L/D at least for $\pm$1° of the design angle. The USP04 has a maximum L/D ratio of 110.8 at 8° (design angle) and a corresponding C_l of 1.63. SG6043 still has the highest L/D ratio of 118.13 at 4.5°.

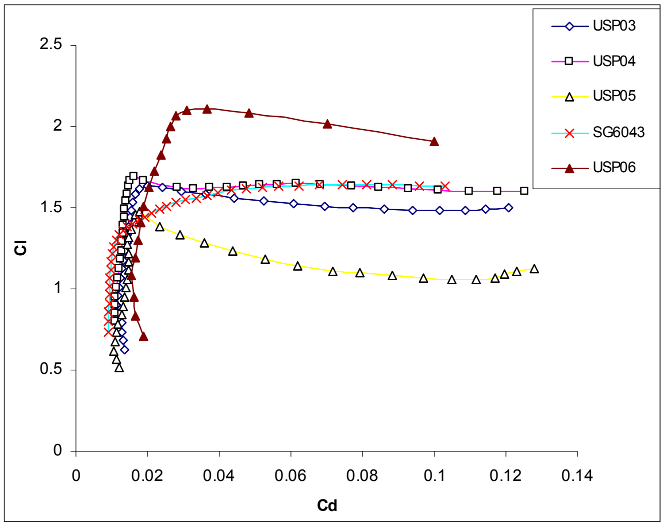

Fig 6: Drag polars for airfoils at Re=300,000

All USP0x airfoils have poor L/D at low alfa compared to SG6043. However all of the optimized airfoils have higher L/D values after 6°. The USP06 maintains L/D of around 75 after 8° while SG6043's L/D continues to drop at this angle.

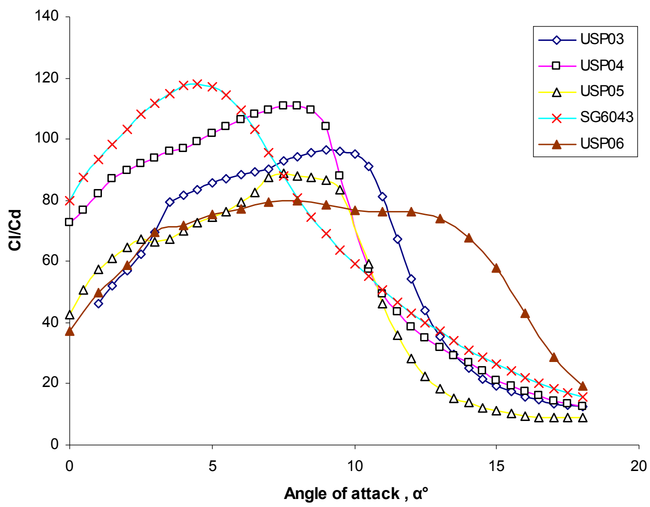

Fig 7: Efficiency (L/D) of the airfoils at Re=300,000

CFD analysis was carried out on USP03 to understand the flow over this airfoil. Figure 8 shows the airfoil mesh for 0° angle of attack. Figure 9 shows the streamlines around USP03 for α =`10° and at a Reynolds number of 300,000. Note that the stagnation point has shifted towards the lower surface due to the increased α value. Higher velocities at the leading edge provide higher suction in the direction of rotation.

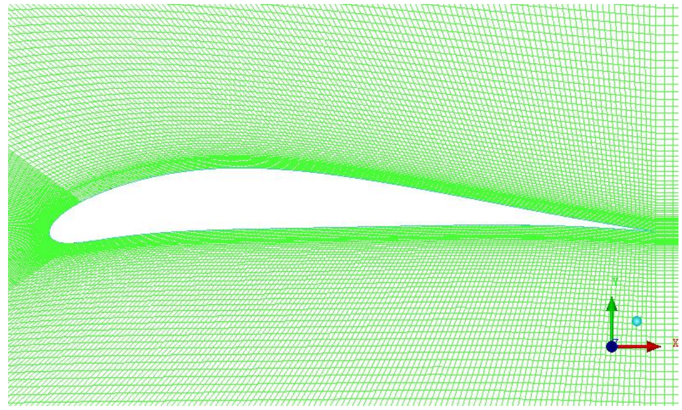

Fig 8: Airfoil grid generation of USP03 in ICEM CFD. The mesh was refined close to the airfoil to capture boundary layer effects**.**

This corresponds to the pressure vectors plotted in XFOIL (Fig 10). The low speed blue region on the top surface close to the trailing edge shows the effects of the boundary layer. This low speed region will grow bigger as the α increases abd gives rise to drag.

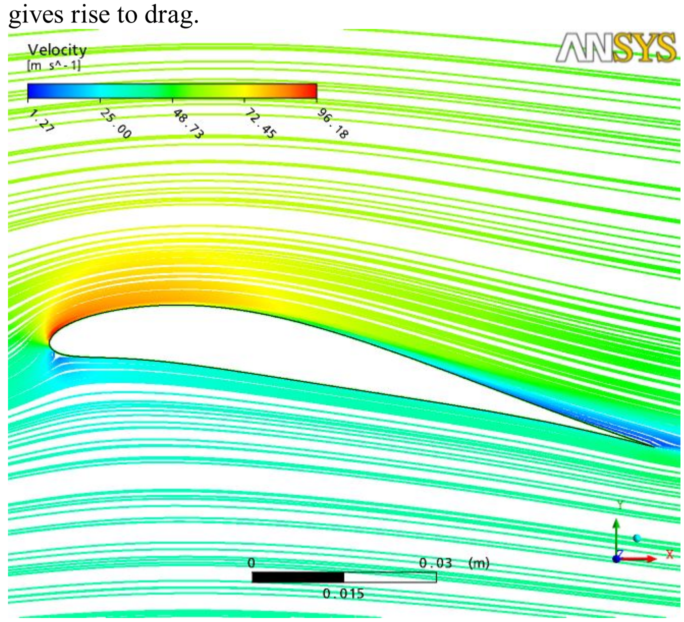

Fig 9: USP03 pressure contours at 10 and Re =300,000. Notice the stagnation point is shifted to the lower surface.

In order to understand the direction of the net force on the airfoil, it is essential to understand what direction the pressure on the airfoil surfaces are pointing in. while maximum lift is desired by having high suction, it must be noted that only a component of the lift actually contributes to the turbines rotation. Lift also contributes to thrust loading on the turbine.

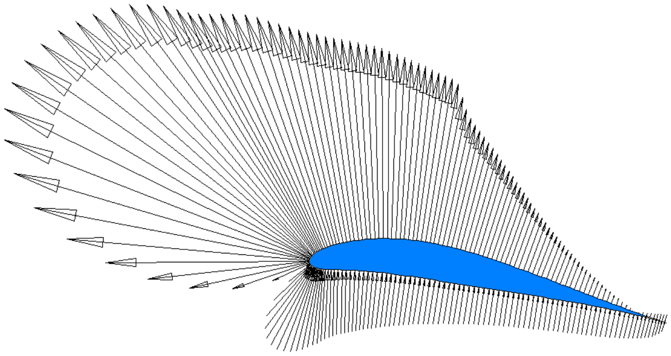

Fig 10: Cp vectors derived from XFOIL show high suction vectors and majority of vectors point in the direction of rotation.

The upper surface pressure vectors near the leading edge have a large component in the direction of rotation. With the stagnation point lowered, the region for suction on the leading edge is increased as shown in Figure 9. The high suction vectors arise orthogonal to the nose and point in the direction of rotation. The vectors also show the existence of negative drag on and near the nose. The inward curvature on the lower surface just after the stagnation point has suction vectors pointing almost vertically, hence reducing the contribution to drag in this region. Experimental validation of the results showed that in the case of USP06 the lift was over predicted by XFOIL (Fig 11) at higher angles of attack. For USP03 which was optimized for 10° angle of attack, the experimental, CFD and XFOIL results for lift coefficients are similar.

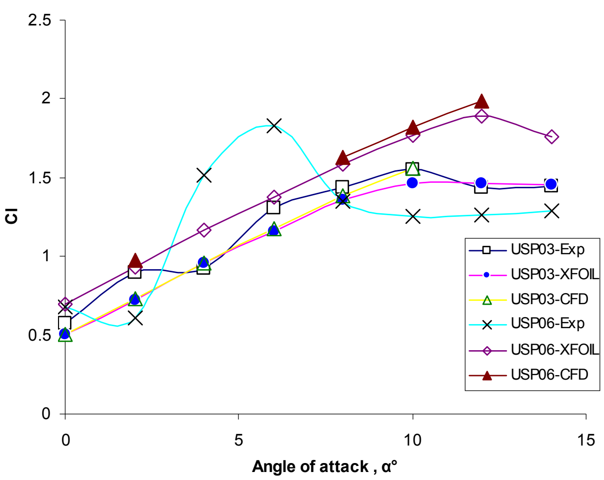

Fig 11: Lift coefficients of USP03 and USP06 from XFOIL, CFD simulations and experiments are compared at Re=200,000.

Experimental results also show the soft stalling of USP03 at 10°. After experimental and CFD investigation it also was observed that both XFOIL and CFD predict lower values of drag coefficient. The experiments points out that while XFOIL is a time efficient solver, correction of the results from the solver are often required to ensure that the airfoil characteristics are not exaggerated.

CONCLUSION

A brief review of airfoil optimization has been presented with emphasis on the common types of parameterization and optimization techniques available. The design of and characteristics of four low Reynolds number airfoils are presented. Using a genetic algorithm optimization scheme coupled with Bezier curve parameterization, four new airfoils were designed to match given objectives. The airfoils are labeled USP03, USP04, USP05 and USP06. While USP03 to USP05 have improved performance between 7 to 10°, USP06 has been designed to accommodate a wide range of flow conditions by maintaining an L/D between 69.5 to 79.6 from 3° to 13°. This airfoil is especially suited for applications near the midsection of small wind turbine blades given its thickness of 14%.

REFERENCES

[1] EWEA, 2010, "Wind Energy - the Facts," Technical Report No. European Wind Energy Association (EWEA),

[2] Giguère, P., and Selig, M. S., 1997, "Low Reynolds Number Airfoils for Samll Horizontal Axis Wind Turbines " Wind Engineering **21** pp. 367-380.

[3] Ahmed, M. R., 2011, "Blade Sections for Wind Turbine and Tidal Current Turbine Applications–Current Status and Future Challenges," International Journal of Energy Research, **36** (7), pp. 829-844.

[4] Ahmed, M. R., Narayan, S., Zullah, M. A., and Lee, Y.-H., 2011, "Experimental and Numerical Studies on a Low Reynolds Number Airfoil for Wind Turbine Blades," Journal of Fluid Science and Technology, **6** (3), pp. 357-371.

[5] Fupeng, H., Yuhong, L., and Zuoyi, C., 2001, "Suggestions for Improving Wind Turbines Blade Characteristics," Wind Engineering, **25** (2), pp. 105-113.

[6] Giguère, P., and Selig, M. S., 1998, "New Airfoils for Small Horizontal Axis Wind Turbines " Journal of Solar Energy Engineering, ASME, **120** pp. 108-114.

[7] Dahl, K. S., and Fuglsang, P., 1998, "Design of the Wind Turbine Airfoil Family Riso-a-Xx," Technical Report No. Riso National Laboratory, Roskilde, Denmark, Roskilde.

[8] Gardner, B. A., and Selig, M. S., "Airfoil Design Using Genetic Algorithm and an Inverse Method. ,"41st Aerospace Sciences Meeting and Exhibit Reno, Nevada,

[9] Holland, J. H., 1975, Adaptation in Natural and Artificial Systems, University of Michigan Press,

[10] Samareh, J. A., "A Survey of Shape Parameterization Techniques "CEA/AIAA/ICASE/NASA Langley International Forum on Aeroelasticity and Structural Dynamics, Williamsburg, VA, 333-343.

[11] Hájek, J., "Parameterization of Airfoils and Its Application in Aerodynamic Optimization "WDS 2007 233-240.

[12] Sobieczky, H., 1998, "Parametric Airfoils and Wings," Notes on Numerical Fluid Mechanics, Viewveg Verlag, **68** pp. 71-88.

[13] Castonguay, P., and Nadarajah, S. K., "Effect of Shape Parameterization on Aerodynamic Shape Optimization,"45th AIAA Aerospace Sciences Meeting and Exhibit,

[14] Shahrokhi, A., and Jahangirian, A., 2007, "Airfoil Shape Parameterization for Optimum Navier–Stokes Design with Genetic Algorithm," Aerospace Science and Technology, Elsevier, **11** pp. 1443-450.

[15] Derksen, R. W., and Rogalsky, T., 2010, "Bezier-Parsec: An Optimized Aerofoil Parameterization for Design," Advances in Engineering Software, Elsevier **41** pp. 923-930.

[16] Zhang, F., Chen, S., and Khalid, M., "Optmization of Airfoil and Wing Using Genetic Algorithm,"23rd Congress of International Council of the Aeronautical Sciences, Toronto, Canada

[17] Bieri, H. P., and Prautzsch, H., 1999, "Preface," Computer Aided Geometric Design, , **16** pp. 579-581.

[18] Grasso, F., "Usage of Numerical Optimization in Wind Turbine Airfoil Design "28th AIAA Applied Aerodynamics Conference - Aerodynamics design: analysis, methodologies & optimization techniques,

[19] Bizzarrini, N., Grasso, F., and Coiro, D. P., "Numerical Optimization for High Efficiency, Low Noise Airfoils,"29th AIAA Applied Aerodynamics Conference, Honolulu, HI, USA,,

[20] Drela, M., 1998, Frontiers of Computational Fluid Dynamics, World Scientific Pros and Cons of Airfoil Optimization

[21] March, A., Willcoxy, K., and Wangz, Q., 2011, "Gradient-Based Multifidelity Optimisation for Aircraft Design Using Bayesian Model Calibration," The Aeronautical Journal **115** (1174), pp. 729-728.

[22] Hazra, S. B., "An Efficient Method for Aerodynamic Shape Optimization,"10th AIAA/ISSMO Multidisciplinary Analysis and Optimization Conference, Albany, New York,

[23] Huang, S. Y., S.Miller, L., and Steck, J. E., "An Exploratory Application of Neural Networks to Airfoil Design,"32nd AlfiiA Aerospace Sciences Meeting and Exhibit, Reno, Nevada,

[24] Khurana, M. S., Winarto, H., and Sinha, A. K., "Application of Swarm Approach and Artificial Neuralnetworks for Airfoil Shape Optimization,"12th AIAA/ISSMO Multidisciplinary Analysis and Optimization Conference Victoria, British Columbia Canada,

[25] Carrese, R., Winarto, H., and Watmuff, J., "User-Preference Particle Swarm Algorithm for Airfoil Design Architecture "27 International Congress of the Aeronautical sciences

[26] Price, K., "Differential Evolution: A Fast and Simple Numerical Optimizer,"Fuzzy Information Processing Society, 1996. NAFIPS. 1996 Biennial Conference of the North American, Vacaville, CA, USA

[27] D. Quagliarella , and Vicini, A., 2001, "Viscous Single and Multicomponent Airfoil Design with Genetic Algorithms," Finite Elements in Analysis and Design, **37** pp. 365-380.

[28] Defalco, I., Balio, R. D., Cioppa, A. D., and Tarantino, E., 1995, "A Parallel Genetic Algorithm for Transonic Airfoil Optimisation," Evolutionary Computation, 1995., IEEE International Conference on, **1** .

[29] Kharal, A., and Saleem, A., 2011, "Neural Networks Based Airfoil Generation for a Given Cp Using Bezier–Parsec Parameterization," Aerospace Science and Technology.

[30] Sivanandam, S. N., and Deepa, S. N., 2008, Introduction to Genetic Algorithms Springer,

[31] Beasley, D., Bull, D. R., and Martin, R. R., 1993, "An Overview of Genetic Algorithms : Part 1 , Fundamentals 1 Introduction 2 Basic Principles," University Computing **15** pp. 1-16.

[32] Lal, S., Yamada, K., and Endo, S., 2008, Springer Berlin / Heidelberg, Emergent Motion Characteristics of a Modular Robot through Genetic Algorithm,Advanced Intelligent Computing Theories and Applications. With Aspects of Artificial Intelligence.

[33] Drela, M., 1989, Low Reynolds Number Aerodynamics, Lecture Notes in Engineering, Springer-Verlag Xfoil: An Analysis and Design System for Low Reynolds Number Airfoils.

